Variation in stem mortality rates determines patterns of aboveground biomass in Amazonian forests: implications for dynamic global vegetation models

Variation in stem mortality rates determines patterns of aboveground biomass in Amazonian forests: implications for dynamic global vegetation models

Running head: Stem mortality controls Amazon forest biomass

Johnson M.O.[1], Galbraith D.[1], Gloor E.[1], De Deurwaerder H.[2], Guimberteau M.[3,4], Rammig A.[5,6], Thonicke K.[6], Verbeeck H.[2], von Randow C.[7], Brienen R.J.W.[1], Feldpausch T.R.[8], Lopez Gonzalez G.[1], Monteagudo A.[9,] Phillips O.L.[1], Quesada C.A.[10], Christoffersen B.[11], Ciais P.[3], Gilvan S.[7], Kruijt B.[12], Meir P.[11,13], Moorcroft P.[14], Zhang K.[15], Alvarez E.A.[16], Alves de Oliveira A.[10], Amaral I.[10], Andrade A.[10], Aragao L.E.O.C.[8], Araujo-Murakami A.[17], Arets E.J.M.M.[18], Arroyo L.[17], Aymard G.A.[19], Baraloto C.[20], Barroso J.[21], Bonal D.[22], Boot R.[23], Camargo J.[10], Chave J.[24], Cogollo A.[25], Cornejo Valverde F.[26], da Costa L.[27], di Fiore A.[28], Higuchi N.[10], Honorio E.[29], Killeen T.J.[30], Laurance S.G.[31], Laurance W.F.[31], Licona J.[32], Lovejoy T.[33], Malhi Y.[34], Marimon B.[35], Marimon Junior B.[35] , Mendoza C.[36], Neill D.A.[37], Pardo G.[38], Peña-Claros M.[39,40], Pitman N.C.A.[41], Poorter L.[40], Prieto A.[42], Ramirez-Angulo H.[43], Roopsind A.[44], Rudas A.[42], Salomao R.P.[45], Silveira M.[46], Stropp J.[47], ter_Steege H.[48], Terborgh J.[41], Thomas R.[44], Toledo M.[39], Torres-Lezama A.[43], van der Heijden G.M.F.[49], Vasquez R.[9], Vieira I.[45], Vilanova E.[43], Vos V.A.[50,51], Baker T.R.[1]

1. School of Geography, University of Leeds, Leeds, LS6 2QT, UK
2. CAVElab Computational & Applied Vegetation Ecology, Faculty of Bioscience Engineering, Ghent University, Coupure Links 653, B-9000 GENT, Belgium

3. Laboratoire des Sciences du Climat et de l'Environnement (LSCE), IPSL, CEA, CNRS, UVSQ, 91191 Gif-sur-Yvette, France

4. UMR 7619 METIS, IPSL, Sorbonne Universités, UPMC, CNRS, EPHE, 75252 Paris, France

5. TUM School of Life Sciences Weihenstephan, Technische Universität München, Hans-Carl-von-Carlowitz-Platz 2, 85354 Freising, Germany

6. Potsdam Institute for Climate Impact Research (PIK), Telegrafenberg A62, P.O. Box 60 12 03, D-14412 Potsdam, Germany

7. INPE, Av. Dos Astronautas, 1.758, Jd. Granja - CEP: 12227-010, Sao Jose dos Campos - SP, Brasil

8. Geography, College of Life and Environmental Sciences, University of Exeter, Rennes Drive, Exeter, EX4 4RJ, UK

9. Jardín Botánico de Missouri, Prolongacion Bolognesi Mz.e, Lote 6, Oxapampa, Pasco, Peru

10. INPA, Av. André Araújo, 2.936 - Petrópolis - CEP 69067-375 - Manaus -AM, Brasil

11. School of Geosciences, University of Edinburgh, Edinburgh EH9 3FF, UK

12. ESS-CC (Earth System Science-Climate Change), Wageningen-UR PO Box 47, 6700 AA Wageningen, The Netherlands

13. Research School of Biology, Australian National University, Canberra, Australia

14. Department of Organismic and Evolutionary Biology, Harvard University, USA

15. Cooperative Institute for Mesoscale Meteorological Studies, University of Oklahoma, USA

16. Servicios Ecosistemicos y Cambio Climático, Jardín Botánico de Medellín, Medellín, Colombia

17. Museo de Historia Natural Noel Kempff Mercado, Universidad Autonoma Gabriel Rene Moreno, Casilla 2489, Av. Irala 565, Santa Cruz, Bolivia

18. Alterra, Wageningen University and Research Centre, PO box 47, 6700 AA Wageningen, The Netherlands
19. UNELLEZ-Guanare, Programa de Ciencias del Agro y el Mar, Herbario Universitario (PORT), Mesa de Cavacas, Estado Portuguesa, Venezuela 3350
20. International Center for Tropical Botany (ICTB), Department of Biological Sciences, Florida International University, 112200 SW 8th Street, OE 167, Miami, FL 33199, USA
21. Universidade Federal do Acre, Campus de Cruzeiro do Sul, Rio Branco, Brazil
22. INRA, UMR 1137 ‘‘Ecologie et Ecophysiologie Forestiere’’, 54280 Champenoux, France
23. Tropenbos International , P.O. Box 232, 6700 AE Wageningen, The Netherlands
24. Université Paul Sabatier CNRS, UMR 5174 Evolution et Diversité Biologique, bâtiment 4R1, 31062 Toulouse, France
25. Jardín Botánico de Medellín Joaquín Antonio Uribe, Cartagena, Colombia
26. Andes to Amazon Biodiversity Program, Madre de Dios, Perú
27. Universidade Federal do Para, Centro de Geociencias, Belem, CEP 66017-970, Para, Brazil
28. Department of Anthropology, University of Texas at Austin, SAC Room 5.150, 2201 Speedway Stop C3200, Austin, TX 78712, USA
29. Instituto de Investigaciones de la Amazonía Peruana, Av. A. José Quiñones km 2.5, Iquitos, Perú
30. World Wildlife Fund, 1250 24th St NW, Washington, DC 20037, USA
31. Centre for Tropical Environmental and Sustainability Science (TESS) and College of Marine and Environmental Sciences, James Cook University, Cairns, Queensland 4878, Australia
32. Instituto Boliviano de Investigación Forestal, C.P. 6201, Santa Cruz de la Sierra, Bolivia
33. Environmental Science and Policy Department and the Department of Public and International Affairs at George Mason University (GMU), Washington DC, USA.

34. Environmental Change Institute, School of Geography and the Environment, University of Oxford, UK

35. Universidade do Estado de Mato Grosso, Campus de Nova Xavantina, Caixa Postal 08, CEP 78.690-000, Nova Xavantina, MT, Brazil

36. FOMABO, Manejo Forestal en las Tierras Tropicales de Bolivia, Sacta, Bolivia

37. Universidad Estatal Amazónica, Facultad de Ingeniería Ambiental, Paso lateral km 2 1/2 via Napo, Puyo, Pastaza, Ecuador

38. Universidad Autonoma del Beni, Campus Universitario, Av. Ejército Nacional, final, Riberalta, Beni, Bolivia

39. Instituto Boliviano de Investigación Forestal, C.P. 6201, Santa Cruz de la Sierra, Bolivia

40. Forest Ecology and Forest Management Group, Wageningen University, PO Box 47, 6700 AA Wageningen, The Netherlands

41. Center for Tropical Conservation, Duke University, Box 90381, Durham, NC 27708, USA

42. Doctorado Instituto de Ciencias Naturales, Universidad Nacional de Colombia, Colombia

43. Instituto de Investigaciones para el Desarrollo Forestal, Universidad de Los Andes, Mérida, Venezuela

44. Iwokrama International Centre for Rainforest Conservation and Development, 77 High Street Kingston, Georgetown, Guyana

45. Museu Paraense Emilio Goeldi, Av. Magalhães Barata, 376 - São Braz, CEP: 66040-170, Belém, PA, Brazil

46. Museu Universitário, Universidade Federal do Acre, Rio Branco AC 69910-900, Brazil

47. Institute of Biological and Health Sciences, Federal University of Alagoas, Maceió, Brazil

48. Naturalis Biodiversity Center, PO Box, 2300 RA, Leiden, The Netherlands

49. University of Nottingham, School of Geography, Nottingham, NG7 2RD

50. Centro de Investigación y Promoción del Campesinado,regional Norte Amazónico, C/ Nicanor Gonzalo Salvatierra N° 362, Casilla 16, Riberalta, Bolivia

51. Universidad Autónoma del Beni, Riberalta, Bolivia

Corresponding author: Dr Tim Baker, t.r.baker@leeds.ac.uk, +44 (0)113 3438356

Keywords: tropical forest, carbon, productivity, DGVM, forest plots, allometry

Type of paper: Primary Research Article

Abstract

Understanding the processes that determine aboveground biomass (AGB) in Amazonian forests is important for predicting the sensitivity of these ecosystems to environmental change and for designing and evaluating dynamic global vegetation models (DGVMs). AGB is determined by inputs from woody productivity (woody NPP) and the rate at which carbon is lost through tree mortality. Here, we test whether two direct metrics of tree mortality (the absolute rate of woody biomass loss and the rate of stem mortality) and/or woody NPP, control variation in AGB among 167 plots in intact forest across Amazonia. We then compare these relationships and the observed variation in AGB and woody NPP with the predictions of four DGVMs. The observations show that stem mortality rates, rather than absolute rates of woody biomass loss, are the most important predictor of AGB, which is consistent with the importance of stand size-structure for determining spatial variation in AGB. The relationship between stem mortality rates and AGB varies among different regions of Amazonia, indicating that variation in wood density and height/diameter relationships also influence AGB. In contrast to previous findings, we find that woody NPP is not correlated with stem mortality rates, and is weakly positively correlated with AGB. Across the four models, basin-wide average AGB is similar to the mean of the observations. However, the models consistently overestimate woody NPP, and poorly represent the spatial patterns of both AGB and woody NPP estimated using plot data. In marked contrast to the observations, DGVMs typically show strong positive relationships between woody NPP and AGB. Resolving these differences will require incorporating forest size structure, mechanistic models of stem mortality and variation in functional composition in DGVMs.

66 **Introduction**

67

68 Tropical forests are the most carbon-rich and productive of all forest biomes (Pan *et al.*, 2011).
69 The Amazon basin in particular comprises approximately 50% of the world's tropical forests,
70 and therefore any perturbations to this ecosystem will have important feedbacks on both carbon
71 cycling and climate worldwide (Zhao & Running, 2010; Wang *et al.*, 2014). It is therefore
72 important that we understand the processes that determine current patterns of carbon storage
73 and cycling in order to predict how the productivity and carbon stores of these forests will
74 respond to changing environmental conditions.

75

76 Our knowledge of the sensitivity of rainforest ecosystems to environmental change is based on
77 three sources. Firstly, observational data from networks of permanent plots, flux towers, remote
78 sensing and aircraft measurements of greenhouse gas concentrations have demonstrated the
79 sensitivity of these ecosystems to environmental change, particularly in response to drought
80 (e.g. Phillips *et al.*, 2009; Restrepo-Coupe *et al.,* 2013; Gatti *et al.*, 2014). Secondly,
81 experimental manipulations of water stress have probed the mechanisms behind these
82 responses (e.g. Nepstad *et al.*, 2007; da Costa *et al.*, 2010, Rowland *et al.* 2015). Thirdly,
83 process-based ecosystem models, especially dynamic global vegetation models (DGVMs) have
84 been used to explore the future sensitivity of Amazon vegetation to increasing temperatures,
85 carbon dioxide concentrations and water stress (e.g. Galbraith *et al.*, 2010). Coupled with
86 climate models, DGVMs have highlighted the sensitivity (Cox *et al.*, 2004), and more recently,
87 the resilience (Rammig *et al.*, 2010; Huntingford *et al.*, 2013) of Amazonian forests to
88 environmental change. However, observations of aboveground biomass (AGB, Mg ha^{-1}) and
89 woody productivity (the amount of net primary productivity (NPP) allocated to aboveground
90 woody growth: W_P, Mg ha^{-1} yr^{-1}) are still little used to parameterize and evaluate DGVMs (e.g.

Castanho *et al.*, 2013; Delbart *et al.*, 2010), despite substantial progress increasing the spatial distribution of such *in situ* observations (e.g. Feldpausch *et al.*, 2011; Mitchard *et al.*, 2014; Quesada *et al.*, 2012). Integrating the insights from such observational studies into the design, calibration and validation of DGVMs would enhance our ability to make convincing predictions of the future of tropical carbon.

Observational data can either be used to evaluate the outputs of models, or more fundamentally, calibrate and inform the processes that models should aim to include. For example, networks of inventory plots have revealed strong differences in AGB among *terra firme* forests in north-east and south-western Amazonia (Baker *et al.*, 2004; Malhi *et al.*, 2006; Baraloto *et al.*, 2011; Quesada *et al.*, 2012; Mitchard *et al.*, 2014). Such observations have been used to evaluate the predictions of Amazonian forest biomass from both remote sensing (e.g. Mitchard *et al.*, 2014) and DGVM studies (e.g. Castanho *et al.*, 2013). These field observations also yield information about the processes that drive variation in aboveground carbon stocks, which can also be used to evaluate and calibrate DGVMs. For example, the paradigm to emerge from previous analysis of plot data in Amazonia is that there is a positive association between woody NPP and stem mortality rates, linked to a reduction in AGB (Baker *et al.* 2004; Malhi *et al.*, 2004; Quesada *et al.*, 2012). This finding has been used to evaluate the architecture and outputs of DVGMs (Negrón-Juárez *et al.* 2015) and has stimulated attempts to make direct links between mortality and woody NPP in these models (Delbart *et al.*, 2010; Castanho *et al.*, 2013).

115 More generally, observational data are valuable for informing how the fundamental processes
116 that influence AGB should be included in vegetation models. For example, the residence time
117 of woody biomass, τ_w (years), is often used as a measure of mortality in DGVMs and is defined
118 for a forest at steady state as:
119
120 $$\tau_w = \frac{AGB}{W_P} \qquad (1)$$
121
122 This parameter varies almost six-fold among tropical forest plots (Galbraith *et al.*, 2013).
123 However, surprisingly, in several commonly-used vegetation models, this parameter is
124 constant; Galbraith *et al.* (2013) found that 21 of the 27 vegetation models they compared use
125 single, fixed values for this parameter. In addition, observational data suggest that the ultimate
126 cause of variation in tree mortality, W_P and hence AGB is variation in edaphic properties
127 (Quesada *et al.*, 2012). Quesada *et al.* (2012) found that spatial differences in W_P correlated
128 most strongly with total soil phosphorus whereas stem mortality rates correlated with a soil
129 physical structure index which combined soil depth, texture, topography and anoxia. Most
130 DGVMs, however, only include very limited feedbacks between vegetation and edaphic
131 properties. Soil properties such as texture are mainly implemented into DGVMs to
132 parameterise hydraulic processes (e.g. Marthews *et al.*, 2014) and soil structure and nutrient
133 content are rarely considered for other processes such as stem mortality.
134
135 Overall, the aim of this study is to compare how variation in W_P and mortality control variation
136 in AGB in Amazonia using both field observations and four DGVMs, in order to inform the
137 future development of vegetation models. In terms of the analysis of observations, we build on
138 previous work (e.g. Baker *et al.* 2004; Malhi *et al.*, 2004; Malhi *et al.*, 2015) in two ways.
139 Firstly, we compare patterns of AGB with variation in two direct measurements of mortality

140 from each plot: the absolute, stand-level rate of woody biomass loss (W_L; Mg ha^{-1} yr^{-1}) and the
141 rate of stem mortality (μ; % yr^{-1}). Previous studies have used τ_w to examine how mortality
142 influences AGB, (e.g. Malhi *et al.*, 2004; Galbraith *et al.*, 2013; Malhi *et al.*, 2015). However,
143 although τ_w is a useful parameter in the context of vegetation modelling and to partition
144 ecosystem carbon fluxes, its dependency on AGB (see Equation 1) means that this term is not
145 an independent control of aboveground biomass stocks: it is inevitable that AGB is inversely
146 related to τ_w. In addition, as τ_w is defined for a forest at steady state, it cannot be easily related
147 to specific short-term processes, such as droughts, which ultimately cause tree mortality. Here,
148 we therefore test the sensitivity of AGB to direct independent measures of both stand- and
149 stem-level variation in mortality rates, as these measures may ultimately provide a more
150 appropriate basis for modelling mortality in DGVMs.
151
152 Secondly, we greatly extend the spatial coverage of observations. The first large-scale studies
153 of Amazon forest dynamics (Baker *et al.*, 2004; Malhi *et al.*, 2004; Phillips *et al.*, 2004) focused
154 on the western, and central and eastern portion of the basin, but included little data from forests
155 on the Guiana and Brazilian Shields (Fig. 1). These areas, however, have distinctive soils,
156 climate, forest structure and species composition (e.g. ter Steege *et al.*, 2006; Feldpausch *et al.*,
157 2011). Here, we use data from these regions to test whether the paradigm of a positive
158 association between woody NPP and stem mortality rates, linked to a reduction in AGB, is
159 found across the full range of Amazonian forests.
160
161 In terms of the analysis of the DGVMs, we aim firstly to establish the reliability of land
162 vegetation simulation for the Amazon basin by comparison of simulation results with kriged
163 maps of field observations of W_P, mortality and AGB that illustrate the major patterns of
164 variation in these variables. We then test how well the four DGVMs capture these spatial

patterns and the overall magnitude of AGB and W_P. Finally, we explore the relationships between simulated AGB, W_P and τ_w. By comparing our findings from the analysis of the observations and simulation results, we conclude by making recommendations for model developments and data collection that will improve our ability to model Amazonian vegetation carbon stocks.

Materials and methods

Plot observations

We used tree inventory data from permanent sample plots located throughout Amazonia compiled as part of the RAINFOR and TEAM networks to estimate stocks (AGB) and fluxes of carbon (woody NPP, stem and biomass mortality) within Amazonian forest stands (Fig. 1). For analysis of AGB, we used the data for the 413 plots analysed by Mitchard *et al.* (2014) (Fig. 1a). For properties which can only be calculated by observing change over time and thus require more than one census, plots in intact, moist, lowland (<1000 m asl) forest were chosen which had a minimum total monitoring period of two years between 1995 to 2009 inclusive. Data for 167 plots that met these criteria for analysis of dynamic properties were downloaded from ForestPlots.net (Lopez-Gonzalez *et al.*, 2011; Lopez-Gonzalez *et al.*, 2012; Fig. 1b and Table S1) and TEAM (data set identifier codes 20130415013221_3991 and 20130405063033_1587). For this dataset, mean plot size is 1.09 ha, the mean date of the first census is 2000.2 and the mean date of the final census is 2008.5. Mean census interval length is 3.70 years and plot mean total monitoring period is 8.3 years. Most of the plots were monitored for most of the time period: on average, 76 % of plots were being monitored in any given year from 2000-2008 (Fig. S1). All trees with a diameter at breast height (dbh) greater than 10 cm were included in the analyses.

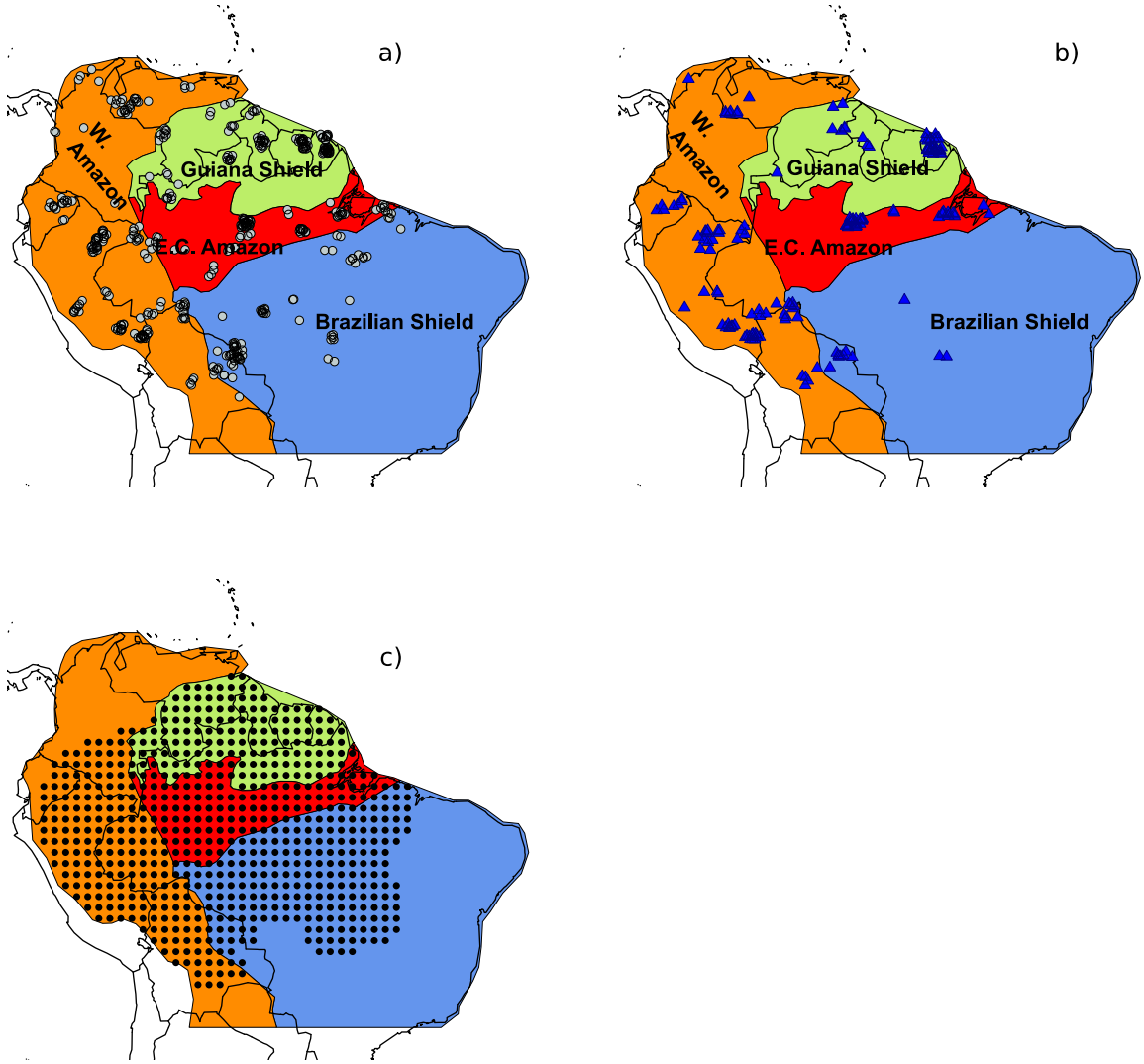

Figure 1. Location of plots used to calculate a) above-ground woody biomass, b) above-ground woody productivity and stem and biomass-based mortality and c) the position of the kriged 1° map grid cells. The Amazon basin is split into regions (shown by different colours) that are defined in Feldpausch *et al.*, (2011). Plot locations are not geographically exact but are offset slightly to improve the visualization of plots which are in very close proximity to each other.

199 Plots were classified into four major Amazon regions that are defined by the nature and
200 geological age of the soil substrate (Fig. 1; Feldpausch *et al.* 2011). The soils and forests of the
201 Guiana and Brazilian Shields have developed on old, Cretaceous, crystalline substrates,
202 whereas, the forests of Western Amazonia are underlain by younger Andean substrates and
203 Miocene deposits (Irion, 1978; Quesada *et al.*, 2010; Higgins *et al.*, 2011). East Central
204 Amazonia contains reworked sediments derived from the other three regions that have
205 undergone almost continuous weathering for more than 20 million years, leading to very
206 nutrient poor soils (Irion, 1978; Quesada *et al.*, 2010). Previous comparative studies have noted
207 substantial differences in forest dynamics between Western and East-Central Amazonia (Baker
208 *et al.*, 2004; Quesada *et al.*, 2012; Baker *et al.*, 2014), but largely excluded forests on the Guiana
209 and Brazilian Shields. This classification therefore allows us to test the impact of including
210 these distinctive forests on Amazon-wide patterns of forest dynamics.
211
212 ***Aboveground biomass***
213 For AGB values, we used the dataset presented by Mitchard *et al.* (2014) and Lopez-Gonzalez
214 *et al.* (2014). In brief, for this dataset, the AGB (Mg ha^{-1}) of each plot was calculated using the
215 Chave *et al.* (2005) moist forest allometric equation which includes measurements of diameter,
216 wood density and height:
217
218 $$AGB = \sum_1^n (0.0509 \rho D^2 H)/1000 \qquad (2)$$
219
220 where D is stem diameter (cm), ρ is stem wood density (g cm^{-3}), H is stem height (m) and n is
221 the number of trees in the stand. We retained the use of this biomass equation for this study,
222 instead of using the recent biomass equation of Chave *et al.* (2014), to provide estimates of W_P
223 that are consistent Mitchard *et al.* (2014). Estimates of AGB for moist tropical forests are in

224 fact similar using either equation (Chave *et al.*, 2014). The height of each tree was estimated
225 from tree diameter using a height-diameter Weibull equation with different coefficients for
226 each region, based on field-measured, height-diameter relationships (Feldpausch *et al.*, 2011).
227 We used this method to estimate tree height, rather than predicting height on the basis of
228 climate as in Chave *et al.*, (2014), because among moist forests in Amazonia, the principal
229 variation in height/diameter allometry is due to the contrast between the particularly tall-
230 statured forests on the Guiana Shield and shorter-statured forest in other regions (Feldpausch
231 *et al.* 2011). This difference is related to the unique species composition of forests on the
232 Guiana Shield rather than variation in climate (Feldpausch *et al.* 2011). The wood density of
233 each tree was assigned on a taxonomic basis from the pan-tropical database of Zanne *et al.*
234 (2009) and Chave *et al.* (2009), following Baker *et al.* (2004). Mean plot wood density values
235 were used when taxonomic information was missing for individual trees.
236
237 To estimate total aboveground woody biomass, we assumed that carbon is 50 % of total dry
238 biomass (Penman *et al.*, 2003) and to account for the unmeasured, small trees (< 10cm), we
239 added an additional 6.2 % of carbon to each of the plots, following Malhi *et al.* (2006). We do
240 not include the unknown contributions from lianas, epiphytes, necromass, shrubs and herbs.
241
242
243
244
245
246
247
248 ***Mortality and productivity***

249 Stem mortality rates were calculated as the exponential mortality coefficient μ (% yr^{-1}; Sheil
250 and May (1996)):

251 $$\mu = \frac{ln(n_0) - ln(n_0 - n_d)}{t} \times 100 \qquad (3)$$

252

253 where n_0 is the number of stems at the start of the census interval, n_d is the number of stems
254 that die in the interval and t is the census interval length. As estimates of mortality rates in
255 heterogeneous populations are influenced by the census interval, we standardised our estimates
256 of μ to comparable census intervals using the equation of Lewis *et al.* (2004). We calculated
257 corrected values of μ for each census interval for each plot in the data set, and calculated
258 average values of μ per plot, weighted by the census interval length.

259

260 Total NPP cannot be calculated from tree inventories as this includes both the growth of the
261 stem as well as litterfall and root production which has only been measured at a relatively small
262 number of Amazonian sites (Malhi *et al.*, 2015). Therefore, we are restricted to calculating W_P,
263 which can be calculated from repeated censuses of tree diameters within inventory plots.
264 Comparable output can be obtained from vegetation models as DGVMs typically partition total
265 aboveground NPP into different carbon pools using various carbon allocation algorithms,
266 ranging from fixed coefficients (e.g. INLAND) to approaches based on resource limitation (e.g.
267 ORCHIDEE). For comparison with measurement data, we used the fraction of simulated
268 aboveground NPP that the models allocate to woody growth. Both the observed measurements
269 and models exclude the contribution to *Wp* that is made by the loss and regrowth of large woody
270 branches. This component is approximately 1 Mg ha^{-1} a^{-1} in Amazonian forests or 10 % of
271 aboveground NPP (Malhi *et al.*, 2009).

272

Estimates of W_P and W_L are influenced by the census interval over which they are calculated, because more trees will recruit and die without being recorded during longer census intervals (Talbot *et al.* 2014). We followed the methods of Talbot *et al.* (2014) for calculating W_P with forest inventory data to correct for this bias (Supplementary information, Appendix S1). Thus, we calculated W_P as the sum of (i) the growth of trees that survive the census period, and the estimated growth of (ii) trees that died during the census interval, prior to their death, (iii) trees which recruited within the interval and (iv) trees that both recruited and died during the census interval. Similarly, to calculate $W_{L,}$ we summed the biomass of trees that die within a census interval with components (ii) and (iv) above.

Analysis of observational data

The current paradigm for Amazonian forests suggests that W_P and μ are positively correlated, and that both correlate negatively with AGB (Malhi *et al.*, 2002; Quesada *et al.*, 2012). We tested whether these relationships are supported by the data from across Amazonia, including plots from the Guiana and Brazilian Shield. Firstly, we explored whether different regions have distinctive patterns of carbon cycling by comparing W_P, W_L, μ and AGB among the four regions using ANOVA. Secondly, we explored the relationships between these terms using generalised least squares regression. We tested whether W_P and either W_L or μ were significantly related to AGB, and whether these relationships differed among the four regions. We accounted for spatial autocorrelation by specifying a Gaussian spatial correlation structure, which is consistent with the shape of the semivariograms for these forest properties across the plot network (Fig. S3). Stem mortality rates and absolute rates of woody biomass loss were log-transformed prior to analysis to ensure the residuals were normally distributed. Model evaluation was performed on the basis of Akaike Information Criterion (AIC) values. Analyses

were carried out using the *nlme* package in R (R Development Core Team 2012, Pinheiro *et al.* 2015).

Model simulations and comparison with observations

We tested how well a range of DGVMs perform for Amazonia by comparing observed AGB, W_P and τ_w to the output from four DGVMs. The DGVMs included in this study are the Joint UK Land Environment Simulator (JULES), v. 2.1. (Best *et al.*, 2011, Clark *et al.*, 2011), the Lund-Potsdam-Jena dynamic global vegetation model for managed Land (LPJmL; Sitch *et al.*, 2003; Gerten *et al.*, 2004; Bondeau *et al.*, 2007), the INtegrated model of LAND surface processes (INLAND) model (a development of the IBIS model, Kucharik et al., 2000; Costa et al., 2015) and the Organising Carbon and Hydrology In Dynamic EcosystEms (ORCHIDEE) model (Krinner *et al.*, 2005). A brief description of each of the four models and how output data are derived is included in the supplementary information (Appendix S2). The models each followed the standardized Moore Foundation Andes-Amazon Initiative (AAI) modelling protocol (Zhang *et al.*, 2015). The simulated region spanned 88°W to 34°W and 13°N to 25°S. Simulations from each model included a spin-up period from bare ground of up to 500 years with pre-industrial atmospheric CO_2 (278 ppm). The models were then forced by recycling 39 year, 1° spatial resolution, bias-corrected NCEP meteorological data (Sheffield *et al.*, 2006) for 1715 to 2008 with increasing CO_2 concentrations, as in Zhang *et al.* (2015). Fig. S2 shows the spatial distribution of mean meteorological variables for 2000-2008 across the Amazon basin. As well as precipitation, temperature and short-wave radiation we also show maximum cumulative water deficit (MWD), calculated from monthly precipitation values to indicate drought severity across the basin, as in Aragao *et al.* (2007). The time period of model output is 2000 to 2008.

To compare simulated woody NPP with observed W_P, corrections were applied to the simulated total woody NPP to calculate aboveground woody NPP only, by assuming a belowground to aboveground allocation ratio of 0.21 (Malhi *et al.*, 2009). In the case of JULES, only a fraction of the NPP is allocated to biomass growth, as the remainder is allocated to 'spreading' of vegetated area - an increase in the fraction of grid cell cover (Cox, 2001). To facilitate comparison with observations and other models, we therefore re-scaled W_P from JULES, retaining the relative allocation to wood but assuming that all of the NPP was used for growth.

We compared model outputs to kriged maps of AGB, W_P and mortality to understand how well the DGVMs captured the major differences in AGB, W_P and mortality across the basin. The forest properties were mapped onto a region defined as Amazonia *sensu stricto* (Eva *et al.*, 2005) which is divided into 1° by 1° longitude-latitude grid cells (Fig. 1c). Model output wass provided for the same grid. The kriged maps were created using ordinary kriging with the *gstat* package in R (Pebesma 2004). To assess the predictive ability of the kriging method we performed a leave-one-out cross validation technique. This involves leaving one site out in turn and performing the kriging using the rest of the observations. The kriging prediction for this location was then compared with the observation. Results from the cross-validation demonstrate that there was no spatial bias in the kriging method (Fig. S4). There was also no tendency for the kriging to overestimate or underestimate values for the whole basin. However, the kriging method was not able to capture the few locations with very high mortality values (Fig. S5). This problem is common to any interpolation method which is effectively averaging observed values. The median percentage bias between the leave-one-out cross validation and the measured plot values were 13.6 %, 12.7 % and 23.0 % for AGB, W_P and stem mortality rate respectively.

We do not intend the kriged maps to be a detailed, accurate description of Amazon forest properties: ecological patterns are a mix of smooth gradients (e.g related to climate) and more abrupt boundaries (e.g. related to edaphic properties) that cannot be shown using these methods. Rather, we intend these maps as broad-scale tools to provide a means of evaluating the performance of the vegetation models.

Finally, we compared how well the DGVMs captured the mean and variability in AGB and W_P and τ_w (calculated using average values for W_P and AGB across all grid cells for 2000-2008 from model outputs using equation 1) for grid cells where there is observational data, and contrast the controls on AGB between observations and models in terms of W_P and mortality. We acknowledge that the models will predict a small increase in W_P over the time period of study due to CO_2 fertilisation (~0.35 Mg ha^{-1} a^{-1}; Lewis *et al.* 2009). However, the effect of this process on estimates of τ_w is small.

Results

Observed links between woody biomass, mortality and productivity

There is strong variation in AGB ($F_{3,163}$=72.1, p<0.001), μ ($F_{3,163}$=23.6, p<0.001) and W_P ($F_{3,163}$=22.7, p<0.001) among the four regions, but not W_L ($F_{3,163}$=1.49, ns; Table 1, Fig. 2). Forests on the Guiana Shield are characterized by the highest AGB of all Amazonian forests, associated with low stem mortality rates and high W_P (Fig. 2a-c). East-central Amazon forests also have comparatively high AGB and similar, very low stem mortality rates. However, W_P is lower in these sites (Fig. 2b). Compared to these regions, forests in the western Amazon and on the Brazilian Shield have lower AGB. However, the lower biomass in these two regions is associated with different patterns in W_P. In the western Amazon, the lower biomass values high

370 W_P (Fig. 2a-c). In contrast, the particularly low biomass forests of the Brazilian Shield have
371 high rates of stem mortality and low W_P (Fig. 2a-c).
372
373 Analysis of the relationships using generalised least squares allows the relative importance of
374 W_P and μ for determining AGB to be explored in more detail. Stem mortality rate is the key
375 parameter that controls variation in AGB (Table 2, Fig. 4c). In contrast, the alternative measure
376 of mortality, W_L, is not related to AGB (Fig. 4b): all models including stem mortality rates,
377 rather than W_L, show substantially better fit and lower AIC values (Table 2). The effect of stem
378 mortality rate on AGB also differs among regions (Fig. 4c).
379
380 For example, for a stem mortality rate of 1.5 % yr^{-1}, forests on the Guiana Shield store
381 approximately 75 % more carbon as (aboveground) wood than forests on the Brazilian Shield
382 (Fig. 4c). Importantly, the relationship between AGB and stem mortality rates is not because
383 there is a correlation between AGB and stem number these two variables are unrelated (Fig.
384 S8). In addition, the strength of the relationship between AGB and stem mortality rates varies
385 among regions: the slope of this relationship is comparatively shallow among the plots in
386 western Amazonia (Fig. 4c). Finally, W_P is significantly positively correlated with variation in
387 AGB, although the relationship is weak (Table 2, Fig. 4a).

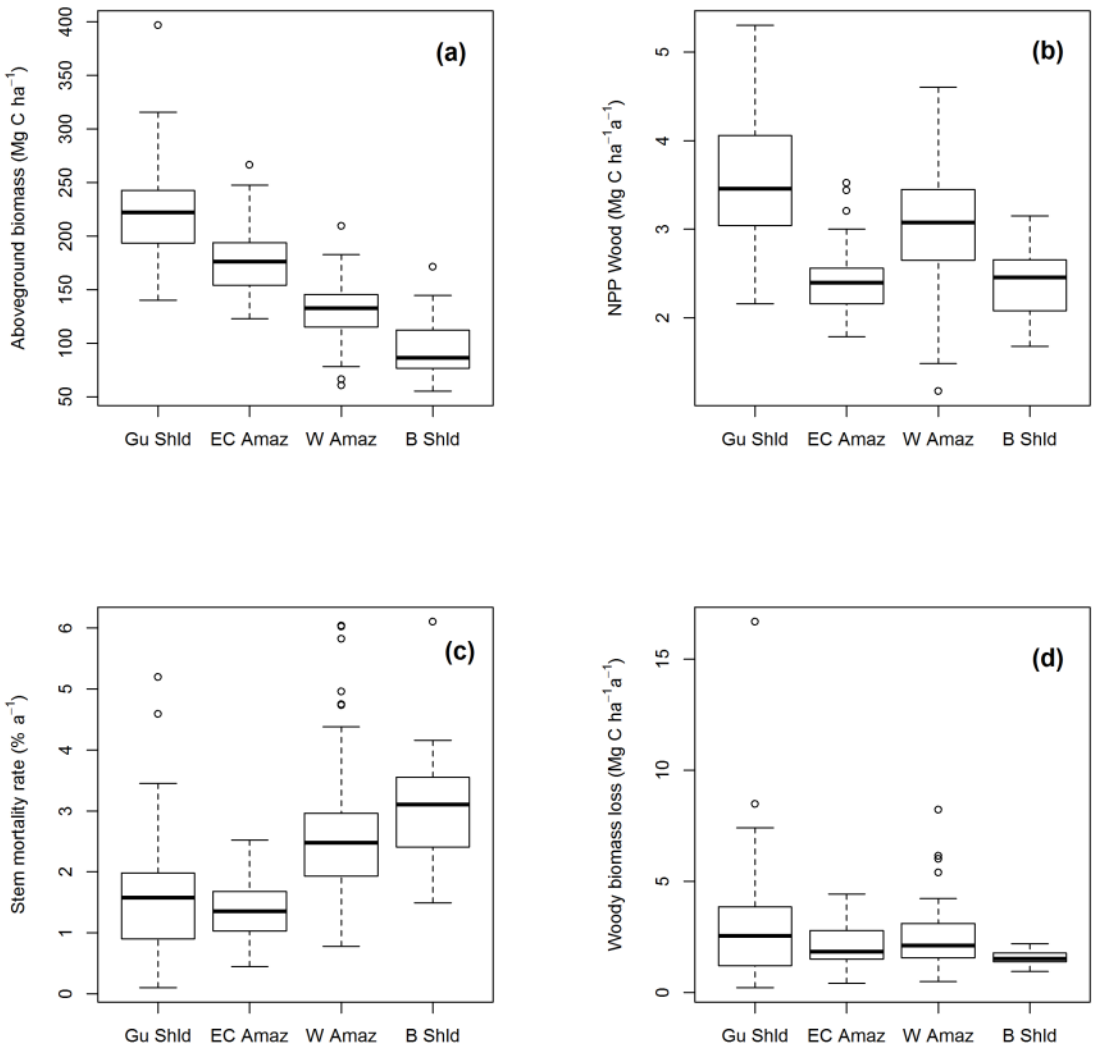

Figure 2. Boxplots of plot measurements of (a) aboveground biomass, (b) aboveground woody productivity, (c) stem mortality rates and (d) absolute rates of woody bomass loss in four regions of Amazonia. Gu Shld = Guiana Shield, EC Amaz = East Central Amazon, W Amaz = Western Amazon, B Shld = Brazilian Shield.

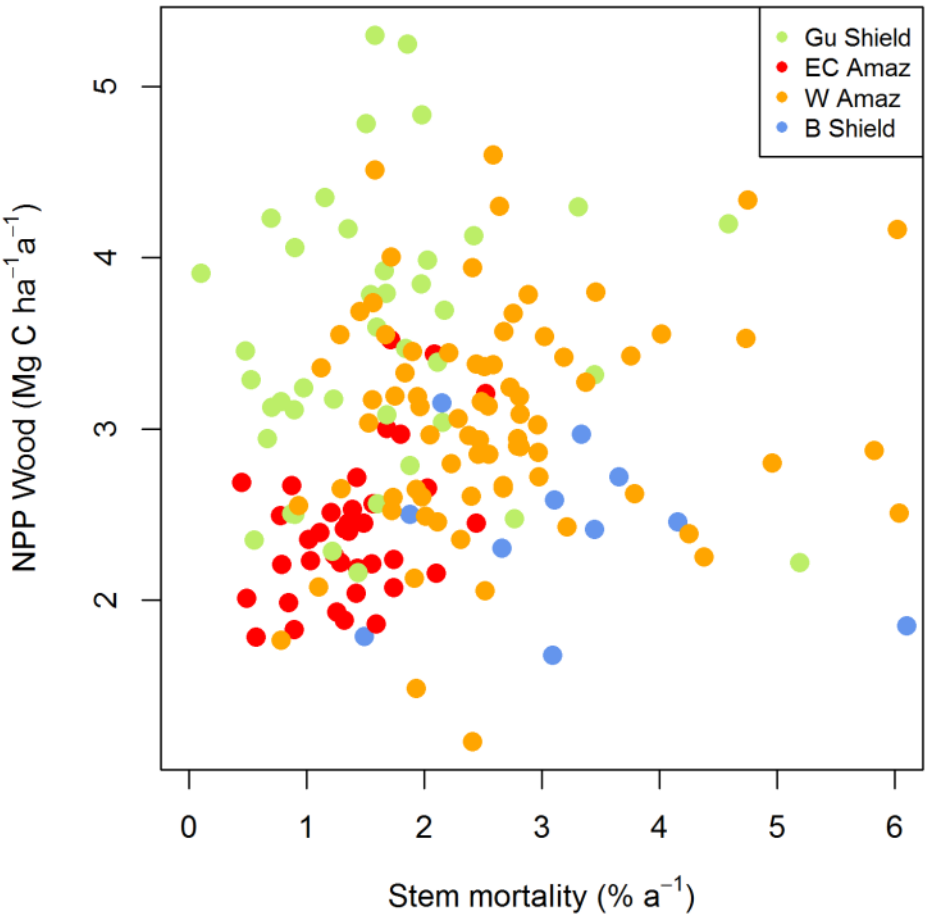

Figure 3. Relationship between woody NPP and stem mortality rates for 167 forest plots in four regions of Amazonia.

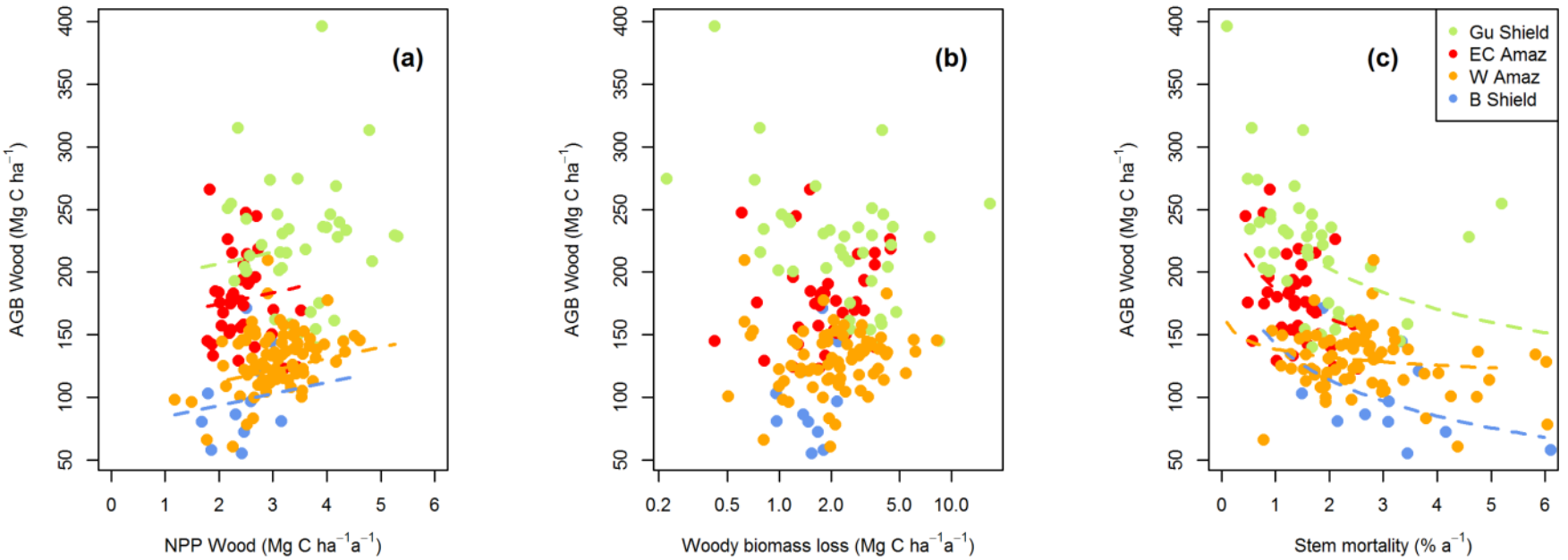

Figure 4. Relationships between AGB and (A) woody NPP, (B) absolute rates of woody biomass loss and (C) stem mortality rates for 167 forest plots in four regions of Amazonia. Lines relate to significant relationships as given by final statistical model in Table 1.

428 **Table 1.** Observed forest properties (mean ± SE) calculated from plot data for each region of Amazonia.

	Basin	**Guiana Shield**	**East central Amazon**	**Western Amazon**	**Brazilian Shield**
Mean aboveground biomass ($Mg\ C\ ha^{-1}$)	153.48 ± 2.82 n=413	211.91 ± 5.03 n=110	167.64 ± 4.95 n=78	126.26 ± 2.38 n=149	107.73±4.48 n=76
Mean aboveground woody productivity ($Mg\ C\ ha^{-1}\ yr^{-1}$)	2.97±0.06 n=167	3.51±0.13 n=41	2.41±0.07 n=37	3.06±0.07 n=76	2.40±0.15 n=13
Stem-based mortality rate ($\%\ yr^{-1}$)	1.96±0.08 n=167	1.66±0.16 n=41	1.38±0.08 n=37	2.62±0.12 n=76	3.19±0.38 n=13
Mean aboveground biomass losses ($Mg\ C\ ha^{-1}\ yr^{-1}$)	2.46±0.13 n=167	3.06±0.44 n=41	2.12±0.16 n=37	2.43±0.15 n=76	1.57±0.12 n=13
Mean wood density ($g\ cm^{-3}$)	0.63±0.00 n=413	0.69±0.00 n=110	0.67±0.01 n=78	0.58±0.00 n=149	0.61±0.01 n=76
Basal area ($m^2\ ha^{-1}$)	26.64±5.53 n=413	29.10±0.49 n=110	28.24±0.51 n=78	25.98±0.41 n=149	22.73±0.66 n=76

429 ***Model projections and comparison with observations***

430

431 The comparisons of simulated AGB and aboveground W_P reveal considerable differences both
432 between the individual models and between the models and observations (Table 3, Figs 5 &
433 6). For the whole of the Amazon basin, mean AGB is highest for ORCHIDEE, and lowest for
434 INLAND; in contrast, woody NPP is highest for LPJmL and lowest for JULES (Table 3).
435 Compared to the plots, different models over- and underestimate mean AGB (Table 3).
436 However, the model ensemble mean AGB value (163.87 Mg C ha^{-1}) is close to the observed
437 mean (153.48 Mg C ha^{-1}). In contrast, all models overestimate aboveground W_P compared to
438 the mean for the plots, by between 36 % (JULES) to 234 % (LPJmL; Table 3, Fig. 5). Variation
439 in τ_w inevitably reflects the variation in mean AGB and woody NPP with average values for
440 ORCHIDEE and JULES (27.9 and 33.2 years) approximately twice the values for INLAND
441 and LPJmL (16.7 and 17.5 years).

442

443 There are considerable differences between the observations and the predictions across the four
444 models in the spatial variability of AGB and W_P (Figs 5 & 6). JULES and INLAND both
445 simulate very little spatial heterogeneity in AGB in the Amazon basin, in contrast to the strong
446 pattern in the observations: compared with the observations they simulate a very

447 **Table 2**. Generalised least squares models relating AGB to variation in aboveground woody productivity (W_P) and (A) stem mortality rates (μ),
448 and (B) rates of woody biomass loss (W_P) among 167 plots across four regions of Amazonia. Terms for mortality were log transformed before
449 analysis. All models incorporated a Gaussian spatial error correlation structure to account for spatial auto-correlation. The model with the strongest
450 support is highlighted in bold; this model was used to quantify the relationships in Figure 3.
451

Model	Terms	Interactions	Log likelihood	AIC	Pseudo r squared
(A) Including μ as mortality term					
1	W_P, μ, *Region*		-810.8	1639.6	0.66
2	***W_P, μ, Region***	***μ * Region***	**-805.0**	**1634.0**	**0.68**
3	W_P, μ, *Region*	W_P * *Region*	-808.8	1641.6	0.67
(B) Including W_L as mortality term					
4	W_P, W_L, *Region*		-829.0	1676.1	0.58
5	W_P, W_L, *Region*	W_L * *Region*	-826.7	1677.4	0.59
6	W_P, W_L, *Region*	W_P * *Region*	-826.6	1677.2	0.59

452

Table 3. Basin mean values, standard errors and root mean square error (RMSE) for aboveground wood biomass (AGB (Mg C ha^{-1})) and aboveground woody net primary productivity (woody NPP (Mg C ha^{-1} yr^{-1})) from the plot observations and mean values from four DGVMs for the plot locations. A belowground to aboveground allocation ratio of 0.21 is applied to the DGVM values to convert from total NPP wood to aboveground woody NPP.

	AGB (Obs mean = 153.48)				W_P (Obs mean = 2.97)			
	AGB wood				**AG NPP wood**			
Model	**ORCHIDEE**	**JULES**	**INLAND**	**LPJmL**	**ORCHIDEE**	**JULES**	**INLAND**	**LPJmL**
Model mean	218.00±3.16	137.93±2.09	125.43±1.35	174.10±2.89	7.80±0.10	4.05±0.09	7.46±0.11	9.92±0.10
RMSE	91.84	76.98	61.36	73.65	5.00	1.89	4.73	7.06

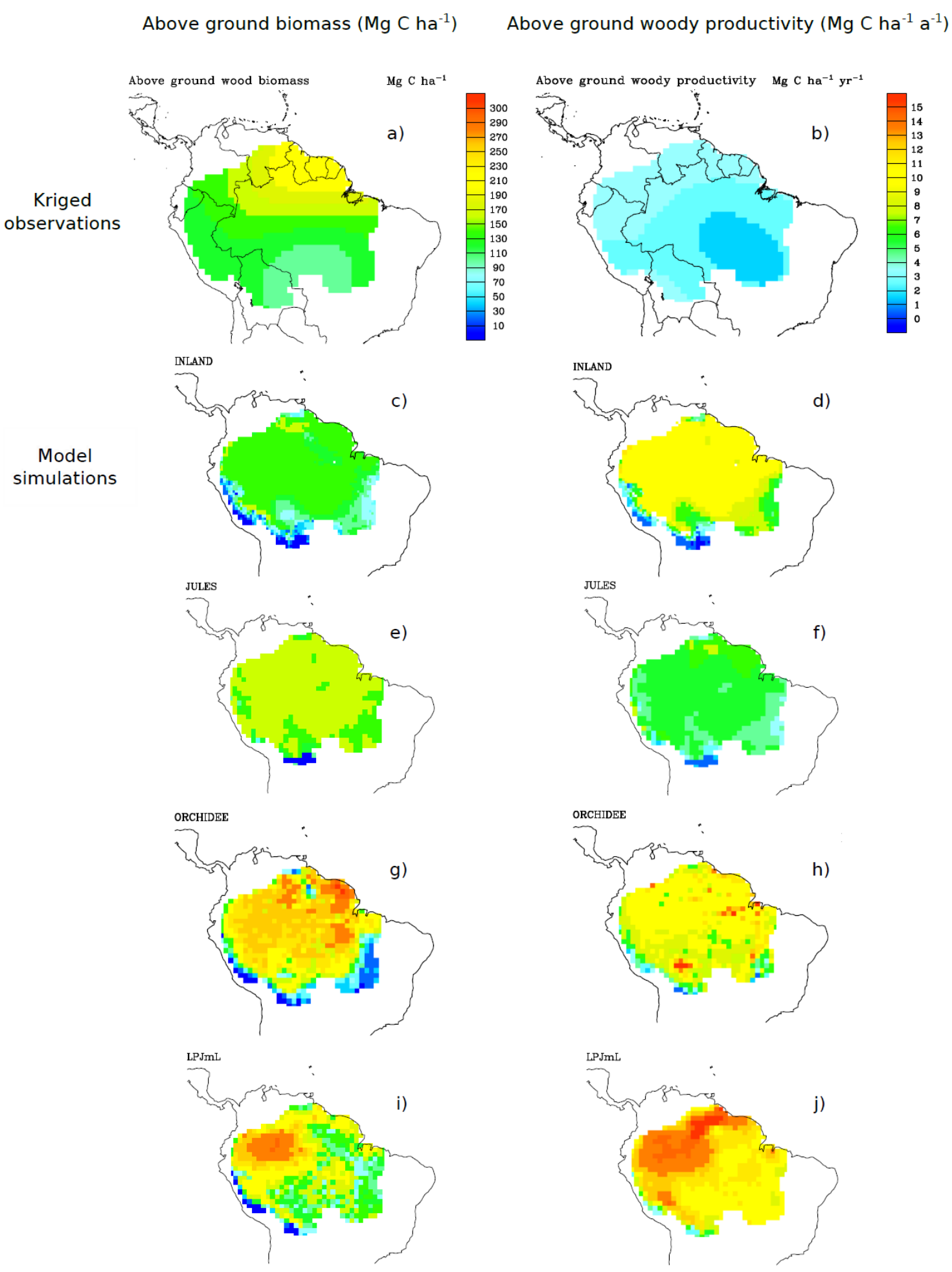
Above ground biomass (Mg C ha-1)
Above ground woody productivity (Mg C ha-1 a-1)
Kriged observations
Model simulations
Above ground wood biomass
Mg C ha-1
300
290
270
250
230
210
190
170
150
130
110
90
70
50
30
10
a)
Above ground woody productivity
Mg C ha-1 yr-1
15
14
13
12
11
10
9
8
7
6
5
4
3
2
1
0
b)
INLAND
c)
INLAND
d)
JULES
e)
JULES
f)
ORCHIDEE
g)
ORCHIDEE
h)
LPJmL
i)
LPJmL
j)

462 **Figure 5** (previous page). Kriged maps of above-ground biomass and woody
463 productivity from RAINFOR forest plot observations and simulated mean aboveground
464 biomass and woody NPP for 2000 – 2008 for four DGVMs.

465

466

467

468

469

470

471

472

473

474

475

476

477

478

479

480

481

482

483

484

485

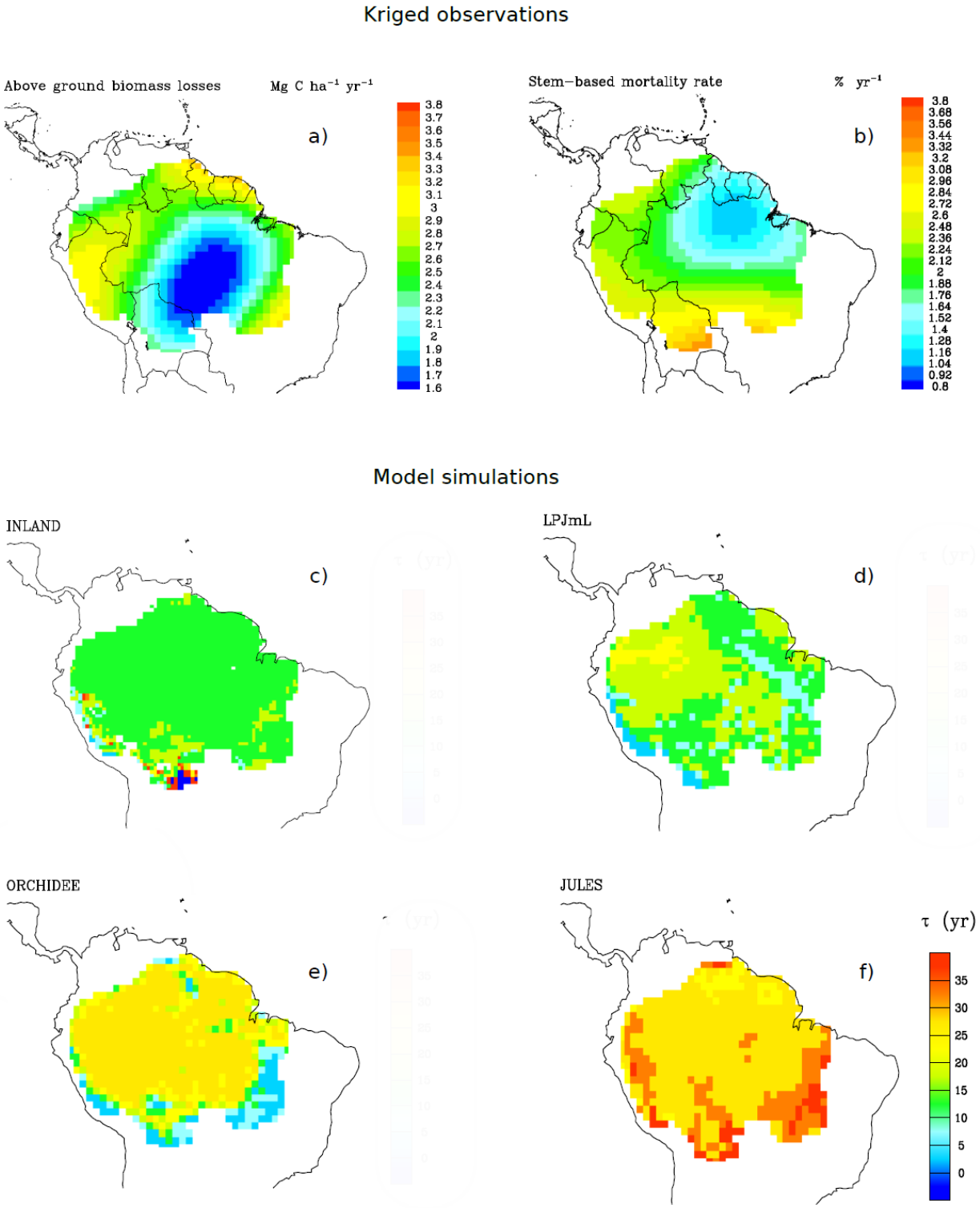

Figure 6. Kriged maps of stem mortality rates and above-ground biomass losses from RAINFOR forest plot observations and simulated mean residence time ($\tau = AGB/W_P$) for 2000 to 2008 for four DGVMs.

narrow range of AGB values and both underestimate the AGB of the Guiana Shield and the basin as a whole (Table 3, Fig. 5c, e). LPJmL and ORCHIDEE display greater variability in their predictions of AGB (Fig. 5g, i). However, LPJmL predicts highest AGB in the north west of the basin in contrast to the observations (Fig. 5i). ORCHIDEE is the only model that provides a reasonable match with the spatial patterns in the observations, but this model still overestimates AGB for most of the basin compared to the plot observations (Table 3, Fig. 5g).

In terms of W_P, LPJmL (Fig. 5j) is the only model that captures the higher observed values in the Guiana Shield and Western Amazon compared with the Brazilian Shield and East Central Amazon (Fig. 5b). In contrast, INLAND, ORCHIDEE and JULES simulate very little variability in W_P across the majority of basin (Fig. 5d, f, h).

For all models, the spatial variation in τ_w is similar to that of AGB (Fig. 6). LPJmL demonstrates the greatest spatial variation in residence times with the highest values found in the north-west of the basin (Fig. 6). JULES and INLAND display little variation in τ_w across the basin. Overall, JULES, LPJmL and INLAND display a much stronger positive relationship between woody NPP and AGB (Fig. 7) than seen in the observations (Fig. 4a), although the form of this relationship varies. In contrast, the relationship predicted by ORCHIDEE matches the variability and form of the relationship from the plot data comparatively well (Fig. 7).

512 Simulated AGB and W_P from all four models show strong relationships with
513 climatological drivers. Correlations between W_P and precipitation are particularly
514 strong for INLAND and LPJmL and all models apart from JULES exhibit strong
515 correlations between rainfall and AGB (Fig. S6). Weaker correlations are observed
516 between temperature and short-wave radiation and simulated W_P and AGB (Fig. S7).

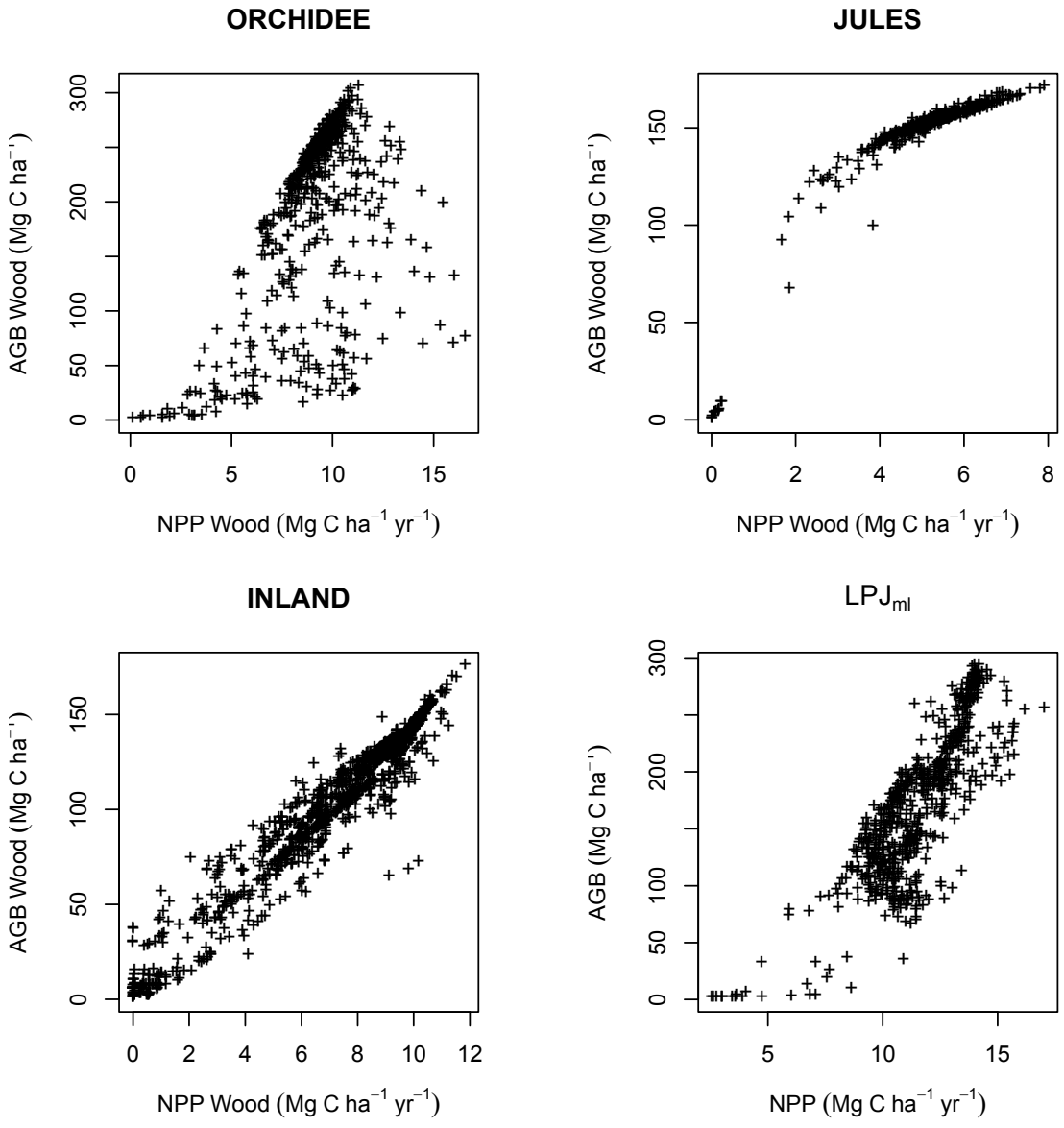

517

518 **Figure 7.** Simulated mean aboveground wood biomass (2000-2008) against simulated
519 mean aboveground woody net primary productivity (2000-2008) for four DGVMs.

520

521 **Discussion**

522 ***Understanding spatial variation in the AGB of Amazon forests***

523

524 Overall, our results extend and enrich the original paradigm concerning the controls on
525 forest dynamics in Amazonia. The previous paradigm described correlated west to east
526 gradients in W_P, stem mortality rates and AGB across the Amazon basin, maintained
527 by a soil-mediated, positive feedback mechanism (Malhi *et al.*, 2004; Quesada *et al.*,
528 2012). Our findings agree that variation in mortality is the key driver of variation in
529 AGB across Amazonian forests (Table 2, Fig. 4). However, our results modify the
530 current paradigm about variation in forest dynamics in Amazonia in four important
531 ways.

532

533 Firstly, the plot data demonstrate that there is no correlation between W_P and stem
534 mortality rates with the new, broader dataset: they vary independently across the basin
535 (Fig. 3). Previous studies have strongly focused on western Amazonia and some east
536 central Amazon sites. However, the inclusion of data from the Guiana Shield in
537 particular demonstrates that low stem mortality rates can also be associated with high
538 W_P (Fig. 3).

539

540 Secondly, our results demonstrate that variation in stem mortality rates, rather than
541 absolute rates of carbon loss, is the key aspect of mortality that determines variation in
542 AGB. The lack of correlation between AGB and absolute rates of biomass loss (Fig.
543 4b) is somewhat surprising: for a forest stand at approximately steady state, we might
544 expect this relationship to at least mirror the weak correlation between mortality and
545 stand W_P (Fig. 4a). This result may be because estimates of absolute AGB loss are

546 subject to greater sampling error than W_P due to stochastic variation in tree mortality
547 (e.g. see wide variation in values on the *x* axis of Fig. 4b). Sampling over longer time
548 intervals may reveal stronger correlations between absolute rates of biomass loss and
549 AGB.
550
551 In contrast to these patterns for absolute rates of loss of biomass, there are strong
552 relationships between stem mortality rates and AGB (Fig. 4c). This result suggests that
553 variation in the numbers and diameters of trees that die in different locations is
554 ultimately a key control on AGB: high rates of stand-level biomass loss and W_P can be
555 associated with high AGB if stem mortality rates are low, and biomass loss is
556 concentrated in a few large trees, but can also be associated with comparatively low
557 AGB if stem mortality rates are high, and mortality is concentrated in a larger number
558 of smaller trees (Fig. 4). Stem mortality rates may influence AGB because they affect
559 the size structure of forests: demographic theory demonstrates how higher stem
560 mortality rates are associated with a steeper slope of tree size/frequency distributions
561 and therefore fewer large trees (Coomes *et al.*, 2003; Muller-Landau *et al.*, 2006). In
562 turn, variation in the number of large trees is a key predictor of spatial variation in
563 biomass among forest plots (e.g. Baker *et al.*, 2004; Baraloto *et al.*, 2011). Importantly,
564 this result indicates that incorporating stem diameter distributions within modelling
565 frameworks will be important for obtaining accurate predictions of AGB.
566
567 Thirdly, our results resolve a paradox in the original paradigm - that W_P showed a slight
568 negative correlation with AGB (Malhi, 2012). Here, with a broader range of sites, the
569 expected positive correlation is found, although the strength of the relationship remains
570 weak (Fig. 4a). Positive correlations between AGB and W_P are a feature of the output

571 of DGVMs (e.g. Fig. 7). This analysis, at least to an extent, brings one aspect of the
572 models in line with the data, although the strength of the observed relationship is much
573 weaker than for the model simulations (Figs 4a & 7).
574
575 Fourthly, the vertical offsets of the relationship between μ and AGB among regions
576 suggest that variation in the identity and height/diameter allometry of trees in different
577 parts of Amazonia is also important for understanding variation in AGB. For example,
578 observations from plots on the Guiana Shield show that these forests have very high
579 AGB values for a given stem mortality rate (Fig. 4c), associated with surprisingly high
580 W_P (Fig. 4a). This result implies that AGB is concentrated within trees with greater
581 heights and/or higher wood density in these forests compared to other regions. A
582 combination of good soil structural properties that promotes low stem mortality rates,
583 and relatively high soil phosphorus concentrations that promote high productivity
584 (Quesada *et al.*, 2012) could conceivably allow these forests to attain the combination
585 of high basal area, tree heights and wood density that results in particularly high AGB.
586 Comparatively high levels of soil fertility are possible as this region may receive
587 significant additions of inorganic phosphorus and other mineral nutrients from dust
588 deposits; this region of the Amazon is believed to receive the highest amounts of dust
589 from Saharan Africa (Mahowald *et al.*, 1999; Mahowald *et al.*, 2005). Alternatively,
590 the greater heights, wood density and W_P of these forests may be related to their
591 distinctive composition; these forests contain a high proportion of stems of large-
592 statured species of Leguminosae (ter Steege *et al.*, 2006). These species may achieve
593 greater phosphorus-use efficiency during photosynthesis or allocate a greater
594 proportion of NPP to woody growth – both are processes that lead to higher AGB
595 forests (Malhi, 2012). Variation in species composition – or the effect of

596 'biogeography' - related to historical patterns of species dispersal over long timescales
597 is known to be a factor in determining the high AGB and W_P of forests in Borneo
598 compared to Amazonia (Banin *et al.*, 2014). Similar processes may also be important
599 within Amazon forests.
600
601 Conversely, forests on the Brazilian Shield towards the southern margins of Amazonian
602 forests have particularly low AGB for a given stem mortality rate, associated with
603 generally low values for W_P and high values of μ (Marimon *et al.*, 2014; Fig. 4). Such
604 low woody productivity, high stem mortality rates and potentially low stature forest in
605 these locations is likely to be caused by moisture stress and/or fire (Phillips *et al.*, 2009;
606 Brando *et al.*, 2014): towards the southern margins of Amazonia, AGB approximately
607 halves with a doubling in moisture stress quantified using the maximum climatological
608 water deficit (Malhi *et al.*, 2015).
609
610 Overall, our findings emphasise the pre-eminent role of variation in stem mortality rates
611 for controlling AGB, but indicate that variation in woody NPP is also important. They
612 also emphasise how the links between AGB, tree growth and mortality are modified by
613 species composition and the allocation of carbon to dense or light wood, or growth in
614 height (Fig. 4c). Clearly, more comprehensive analyses of these sites including
615 environmental data (cf Quesada *et al.*, 2012) are required to tease apart the underlying
616 drivers of these patterns. Additional data from low AGB forests in stressful
617 environments across Amazonia, such as on white sand or peat (Baraloto *et al.*, 2011;
618 Draper *et al.*, 2014) would also be valuable. Such low AGB forests have typically been
619 excluded from ecosystem monitoring but may prove particularly informative to
620 constrain the form of the relationships between W_P, stem mortality rates and AGB.

621

622 Finally, our results suggest that the sensitivity of AGB to variation in stem mortality
623 rates is greater in high AGB forests which have the lowest stem mortality rates (Fig.
624 4c). Increasing mortality rates are a feature of many threats faced by tropical forests,
625 whether driven by increased growth, drought or fire, and extrapolations from forest plot
626 data have been used to argue that such increases may substantially reduce the carbon
627 stocks and carbon sink potential of these ecosystems (e.g. Lewis, 2006; Brienen *et al.*,
628 2015). Our results indicate that forests with the highest AGB values will be most
629 sensitive to a given increase in stem mortality rates (Fig. 4c). In addition, our results
630 suggest that there may be regional differences in the sensitivity of the carbon stocks of
631 Amazonian forests to changing stem mortality rates. For example, increases in stem
632 mortality rates in the Guianas will not lead these forests to become structurally identical
633 to western Amazon forests; they will follow their own trajectory related to their
634 distinctive composition (Fig. 4c).

635

636 ***Understanding spatial patterns in model simulations***

637

638 Simulated AGB in the four DVGMs depends on the balance of woody NPP and losses
639 due to the turnover of woody tissue, 'background' mortality, specific processes such as
640 drought, or more generic 'disturbance' (Table 4). Here, we consider how these models
641 simulate woody NPP and mortality in order to understand simulated patterns of AGB.
642 Woody NPP in JULES is not responsive to the climate and soil variability across the
643 Amazon basin and this model therefore simulates very

644 **Table 4.** Comparison of woody biomass mortality/turnover schemes used by the four DGVMs of this study. Where specific values are provided,

645 these relate to the dominant PFT assumed by the models over our area of study.

646

647

	INLAND	JULES	LPJmL	ORCHIDEE
1. Turnover of woody tissue				
Fixed/variable	Fixed	Fixed	Fixed	Fixed
Woody turnover time	25 years	200 years		30 years
2. Background disturbance rate				
Yes/No?	Yes	Yes	No	No
% a^{-1}	0.05	0.05		
3. Specific drivers of mortality				
Negative carbon balance	No	No	Yes	No
Fire	Yes	No	Yes	No
Drought	No	No	Yes	No
Competition	No	No	No	No
References	Kucharik *et al.* 2000	Clark *et al*. 2011	Sitch *et al.* 2003	Delbart *et al.* 2010

648

649 little variation in W_P across the Amazon (Fig. 5). This pattern translates into little
650 variation in simulated AGB because mortality is essentially constant in JULES (Table
651 XXX) and simulated τ_w is largely invariant (Figs. 5 & 6). As a result there is a positive
652 relationship between simulated AGB and NPP for this model (Fig. 7). However,
653 interestingly, the relationship between AGB and NPP in JULES is non-linear and
654 suggests that there is an upper limit to the amount of AGB that can be simulated in
655 JULES. This arises from the particular allocation scheme used in JULES (Cox, 2001).
656 In JULES, NPP is partitioned into biomass growth of existing vegetation or into
657 'spreading' of vegetated area. This partitioning into growth/spreading is regulated by
658 LAI so that as LAI increases, less NPP is allocated to biomass growth. In this
659 formulation, a maximum LAI value is prescribed which effectively sets a cap on
660 biomass growth in the model, as at this point all of the NPP is directed into 'spreading'
661 and none of it into growth of the existing vegetation. When a PFT occupies all of the
662 available space in a gridcell and therefore cannot expand in area, all of the NPP
663 effectively enters the litter via an assumed 'self-shading' effect (Huntingford *et al.*,
664 2000).
665
666 INLAND simulates slightly more variation in W_P across the basin than JULES.
667 However most of this variation is observed at the basin fringes, which may be explained
668 by INLAND's non-linear relationship between W_P and rainfall; where annual rainfall
669 exceeds 2 m yr^{-1}, simulated W_P does not vary with changes in precipitation (Fig. S6).
670 As a result there is a very strong relationship between AGB and NPP (Fig. 7), and AGB
671 varies little across Amazonia, similar to JULES (Fig. 5).
672

673 Productivity in LPJmL is much more strongly related to rainfall and MWD than either
674 JULES or INLAND (Fig. S6), which is consistent with previous studies that have
675 shown LPJ to be more sensitive to soil moisture stress than other models such as
676 MOSES-TRIFFID, the precursor model to JULES (Galbraith *et al.*, 2010). As a result,
677 we observe more spatial variation across the basin in W_P. More generally, mortality is
678 also more complex in this model and is a function of competition, negative growth, heat
679 stress and bioclimatic limits, and includes disturbance from fire (Table 1; Sitch *et al.*,
680 2003). As result, in contrast to the other models, there are correlations between τ_w,
681 rainfall and MWD in LPJmL (Fig. S6) resulting in substantial spatial variation in AGB
682 and the highest AGB values in the wet, north west of the basin.
683
684 ORCHIDEE also demonstrates spatial variation in W_P which is non-linearly correlated
685 with rainfall (Fig. S6). Carbon residence times and AGB in ORCHIDEE are similarly,
686 but more strongly, correlated with rainfall and MWD than W_P, and as a result, there is
687 greater variability in the relationship between AGB and NPP for this model (Fig. 11),
688 and greater spatial variation in AGB (Fig. 5).
689
690 ***How can we improve simulations of spatial variation in DGVMs based on the***
691 ***observations?***
692
693 A possible explanation for some of the disparities between the observations and model
694 simulations are differences in how disturbance influences both datasets: the forest plots
695 will experience the full range of disturbances that occur in natural forest, whilst the
696 simulations are limited to reflecting the effect of modelled processes. However, in
697 broad terms, the degree and intensities of disturbance are likely to be comparable:

698 amongst the DVGMs in this study, mortality at a background rate due to tree
699 senescence, competition, drought and externally forced disturbance (Table 4). Rare but
700 intense, large-scale disturbances related to blowdowns are excluded from the
701 simulations and such disturbances can have a substantial landscape-scale effects
702 (Chambers *et al.* 2013). However, their extreme rarity and patchiness at a regional scale
703 makes it unlikely that they substantially alter or determine broad-scale patterns of forest
704 structure and dynamics (Espírito-Santo *et al.* 2014).
705
706 A key finding from the observational data is that variation in stem mortality rates
707 determines spatial variation in AGB (Fig. 3). This finding implies that mortality must
708 be modelled on the basis of individual stems, and suggests stem-size distributions are
709 important for predicting variation in AGB. However, the architecture of the DVGMs in
710 this study do not incorporate stem size distributions, or individual-based mortality rates.
711 In contrast, all models in this study employ a fixed value of τ_w (a PFT-specific woody
712 turnover rate, Table 4), to model a background rate of woody biomass loss, related to
713 growth. In the models where these constant terms dominate mortality (e.g.
714 JULES/INLAND), inevitably, the patterns of AGB mirrors those of W_P and do not
715 match the observations. Even in ORCHIDEE which simulates the highest biomass in
716 the northwest of the basin similar to the observations (Fig. 5), this apparent
717 correspondence between the model and observations is not because this model
718 effectively models tree mortality: like JULES and INLAND, ORCHIDEE also employs
719 a constant mortality rate (Table 4; Delbart *et al.*, 2010). In addition, the finding that
720 variation in stem mortality determines variation in AGB, implies that introducing
721 simple relationships between mortality and W_P, such as linking τ_w to NPP (Delbart *et*
722 *al.*, 2010) will not improve predictions for the whole basin. For example, the forests of

723 the Guiana Shield, where forests have high W_P and high AGB but low stem mortality
724 rates, will not be accurately modelled using the technique employed by Delbart *et al.,*
725 2010).
726
727 A second key reason for discrepancies between the observations and models is that the
728 key processes driving variation in the observations differ from the modelled processes.
729 For example, when mortality is included as a dynamic process in the DGVMs, such as
730 in LPJmL, mortality strongly reflects the variability in that process –due to moisture
731 stress across the basin in the context of LPJmL. In contrast, stem mortality rates in
732 Amazonian plots ultimately strongly respond to edaphic properties such as soil physical
733 properties (Quesada *et al.*, 2012).
734
735 These findings suggest several ways in which vegetation models could be developed.
736 Firstly, mortality needs to be effectively incorporated in these models, preferably
737 through incorporating stem mortality rates (μ), rather than average carbon residence
738 times (τ_w), as a means of modelling the loss of woody carbon. The process of stem
739 mortality is much more amenable for linking with the ultimate drivers of tree death,
740 such as hydraulic failure, and is the key driver of variation in the size structure and
741 AGB of Amazonian forests. We note that there have been positive advances in
742 modelling mortality processes more mechanistically in DGVMs (e.g. Fisher *et al.*,
743 2010) and that there is considerable focus at present in improving the representation of
744 vegetation dynamics in DGVMs (e.g. Verbeeck *et al.*, 2011; De Weirdt *et al.*, 2012;
745 Castanho *et al.*, 2013; Haverd *et al*. 2014; Weng *et al*. 2015). Secondly, DGVMs need
746 to focus on including more functional diversity and variation in height/diameter
747 relationships to capture regional differences in the carbon dynamics of Amazon forests.

748 Thirdly, mortality processes need to be linked to edaphic properties such as a measure
749 of soil structure/stability, and W_P to spatially varying soil nutrients to ensure that not
750 only climate stress influences spatial variation of AGB that is predicted by DGVMs.
751 Finally, our study highlights the importance of size structure in shaping forest
752 dynamics. To model tropical forest dynamics effectively, 'average individual'
753 approaches which do not account for size distributions in tropical forests are
754 insufficient. Several different aspects of these recommendations are already being
755 implemented (e.g. Fyllas *et al.*, 2014; Sakschewski *et al.*, 2015) and we look forward
756 to testing the predictions of the next generation of vegetation models against baseline
757 datasets of forest structure and dynamics.
758
759
760
761
762
763
764
765
766
767
768
769
770
771
772 **Acknowledgements**

This paper is a product of the European Union's Seventh Framework Programme AMAZALERT project (282664). The field data used in this study is from the RAINFOR network, which has been supported by a Gordon and Betty Moore Foundation grant, the Eu Programme projects 283080, 'GEOCARBON'; and 282664, 'AMAZALERT'; ERC grant 'Tropical Forests in the Changing Earth System'), and Natural Environment Research Council (NERC) Urgency, Consortium and Standard Grants 'AMAZONICA' (NE/F005806/1), 'TROBIT' (NE/D005590/1) and 'Niche Evolution of South American Trees' (NE/I028122/1). Additional data were included from the Tropical Ecology Assessment and Monitoring (TEAM) Network - a collaboration between Conservation International, the Missouri Botanical Garden, the Smithsonian Institution and the Wildlife Conservation Society, and partly funded by these institutions, the Gordon and Betty Moore Foundation, and other donors. Fieldwork was also partially supported by Conselho Nacional de Desenvolvimento Científico e Tecnológico of Brazil (CNPq), project Programa de Pesquisas Ecológicas de Longa Duração (PELD-403725/2012-7). A.R. acknowledges funding from the Helmholtz Alliance 'Remote Sensing and Earth System Dynamics'; L.P., M.P.C. E.A., and M.T. are partially funded by the EU FP7 project 'ROBIN' (283093), with co-funding for E.A. from the Dutch Ministry of Economic Affairs (KB-14-003-030); O.L.P. is supported by an ERC Advanced Grant and is a Royal Society-Wolfson Research Merit Award holder. T.R.B. acknowledges financial support from a Leverhulme Trust Research Fellowship (2015-2017).

Model simulations

References

798 Aragao LEO, Malhi Y, Roman-Cuesta RM, Saatchi S, Anderson LO, Shimabukuro
799 YE (2007) Spatial patterns and fire response of recent Amazonian droughts.
800 *Geophysical Research Letters,* **34**, LO7701.
801 Baker TR, Pennington RT, Magallon S *et al.* (2014) Fast demographic traits promote
802 high diversification rates of Amazonian trees. *Ecology Letters,* **17**, 527-536.
803 Baker TR, Phillips OL, Malhi Y *et al.* (2004) Variation in wood density determines
804 spatial patterns in Amazonian forest biomass. *Global Change Biology,* **10**,
805 545-562.
806 Banin L, Lewis SL, Lopez-Gonzalez G *et al.* (2014) Tropical forest wood production:
807 a cross-continental comparison. *Journal of Ecology*, **102**, 1025-1037.
808 Baraloto C, Rabaud S, Molto Q *et al.* (2011) Disentangling stand and environmental
809 correlates of aboveground biomass in Amazonian forests. *Global Change*
810 *Biology,* **17**, 2677-2688.
811 Best M, Pryor M, Clark D *et al.* (2011) The Joint UK Land Environment Simulator
812 (JULES), model description–Part 1: energy and water fluxes. *Geoscientific*
813 *Model Development,* **4**, 677-699.
814 Bondeau A, Smith PC, Zaehle S *et al.* (2007) Modelling the role of agriculture for the
815 20th century global terrestrial carbon balance. *Global Change Biology,* **13**,
816 679-706.
817 Brando PM, Balch JK, Nepstad DC *et al.* (2014) Abrupt increases in Amazonian tree
818 mortality due to drought–fire interactions. *Proceedings of the National*
819 *Academy of Sciences,* **111**, 6347-6352.
820 Brienen R, Phillips O, Feldpausch T *et al.* (2015) Long-term decline of the Amazon
821 carbon sink. *Nature,* **519**, 344-348.

822 Castanho A, Coe M, Costa M, Malhi Y, Galbraith D, Quesada C (2013) Improving
823 simulated Amazon forest biomass and productivity by including spatial
824 variation in biophysical parameters. *Biogeosciences,* **10**, 2255-2272.
825 Chambers JQ, Negron-Juarez RI *et al.* (2013). The steady-state mosaic of disturbance
826 and succession across an old-growth Central Amazon forest landscape.
827 *Proceedings of the National Academy of Sciences* **110**, 3949-3954.
828 Chave J, Andalo C, Brown S *et al.* (2005) Tree allometry and improved estimation of
829 carbon stocks and balance in tropical forests. *Oecologia,* **145**, 87-99.
830 Chave J, Coomes D, Jansen S, Lewis SL, Swenson NG, Zanne AE (2009) Towards a
831 worldwide wood economics spectrum. *Ecology Letters,* **12**, 351-366.
832 Chave J, Réjou-Méchain M, Búrquez A *et al.* (2014) Improved allometric models to
833 estimate the aboveground biomass of tropical trees. *Global Change Biology,*
834 **20**, 3177-3190.
835 Clark D, Mercado L, Sitch S *et al.* (2011) The Joint UK Land Environment Simulator
836 (JULES), model description–Part 2: carbon fluxes and vegetation dynamics.
837 *Geoscientific Model Development,* **4**, 701-722.
838 Coomes DA, Duncan RP, R.B. A, Truscott J (2003) Disturbances prevent stem size-
839 density distributions in natural forests from following scaling relationships.
840 *Ecology Letters,* **6**, 980-989.
841 Cox PM (2001) Description of the TRIFFID dynamic global vegetation model.
842 Technical Note 24, Hadley Centre, United Kingdom Meteorological Office,
843 Bracknell, UK.
844 Cox PM, Betts R, Collins M, Harris P, Huntingford C, Jones C (2004) Amazonian
845 forest dieback under climate-carbon cycle projections for the 21st century.
846 *Theoretical and Applied Climatology,* **78**, 137-156.

847 Da Costa ACL, Galbraith D, Almeida S *et al.* (2010) Effect of 7 yr of experimental
848 drought on vegetation dynamics and biomass storage of an eastern Amazonian
849 rainforest. *New Phytologist,* **187**, 579-591.
850 De Weirdt M, Verbeeck H, Maignan F *et al.* (2012) Seasonal leaf dynamics for
851 tropical evergreen forests in a process-based global ecosystem model, *Geosci.*
852 *Model Dev.*, **5**, 1091–1108.
853 Delbart N, Ciais P, Chave J, Viovy N, Malhi Y, Le Toan T (2010) Mortality as a key
854 driver of the spatial distribution of aboveground biomass in Amazonian forest:
855 results from a dynamics vegetation model. *Biogeosciences,* **7**, 3017-3039.
856 Draper FC, Roucoux KH, Lawson IT *et al.* (2014) The distribution and amount of
857 carbon in the largest peatland complex in Amazonia. *Environmental Research*
858 *Letters,* **9**, 124017.
859 Espírito-Santo FD, Gloor E *et al.* (2014). Size and frequency of natural forest
860 disturbances and the Amazon forest carbon balance. *Nature Communications*
861 **5**.
862 Eva HD, Huber O, Achard F *et al.* (2005) A proposal for defining the geographical
863 boundaries of Amazonia. *Luxembourg Office for Official Publications of the*
864 *European Communities,* pp 1-38.
865 Feldpausch TR, Banin L, Phillips OL *et al.* (2011) Height-diameter allometry of
866 tropical forest trees. *Biogeosciences,* **8**, 1081-1106.
867 Feldpausch TR, Lloyd J, Lewis SL *et al.* (2012). Tree height integrated into
868 pantropical forest biomass estimates. *Biogeosciences*, **9**, 3381-3403.
869 Fisher R, Mcdowell N, Purves D *et al.* (2010) Assessing uncertainties in a second-
870 generation dynamic vegetation model caused by ecological scale limitations.
871 *New Phytologist,* **187**, 666-681.

872 Fyllas N, Gloor E, Mercado L *et al.* (2014) Analysing Amazonian forest productivity
873 using a new individual and trait-based model (TFS v. 1). *Geoscientific Model*
874 *Development,* **7**, 1251-1269.
875 Galbraith D, Levy PE, Sitch S, Huntingford C, Cox P, Williams M, Meir P (2010)
876 Multiple mechanisms of Amazonian forest biomass losses in three dynamic
877 global vegetation models under climate change. *New Phytologist,* **187**, 647-
878 665.
879 Galbraith D, Malhi Y, Affum-Baffoe K *et al.* (2013) Residence times of woody
880 biomass in tropical forests. *Plant Ecology & Diversity,* **6**, 139-157.
881 Gatti L, Gloor M, Miller J *et al.* (2014) Drought sensitivity of Amazonian carbon
882 balance revealed by atmospheric measurements. *Nature,* **506**, 76-80.
883 Gerten D, Schaphoff S, Haberlandt U, Lucht W, Sitch S (2004) Terrestrial vegetation
884 and water balance—hydrological evaluation of a dynamic global vegetation
885 model. *Journal of Hydrology,* **286**, 249-270.
886 Group GSDT (2000) Global gridded surfaces of selected soil characteristics.
887 International Geosphere-Biosphere Programme, Data and Information System
888 CD-ROM, Oak Ridge National Laboratory Distributed Active Archive Center
889 Oak Ridge, Tennessee.
890 Guariguata, M, Ostertag R (2001) Neotropical secondary forest succession: changes
891 in structural and functional characteristics. *Forest Ecology and Management*
892 **148**, 185-206.
893 Haverd V, Smith B, Nieradzik LP, Briggs PR (2014) A stand-alone tree demography
894 and landscape structure module for Earth system models: integration with
895 inventory data from temperate and boreal forests. *Biogeosciences*, **11**, 4039-
896 4055.

897 Higgins MA, Ruokolainen K, Tuomisto H *et al.* (2011) Geological control of floristic
898 composition in Amazonian forests. *Journal of Biogeography,* **38**, 2136-2149.
899 Huntingford C, Cox P, Lenton T (2000) Contrasting responses of a simple terrestrial
900 ecosystem model to global change. *Ecological Modelling,* **134**, 41-58.
901 Huntingford C, Zelazowski P, Galbraith D *et al.* (2013) Simulated resilience of
902 tropical rainforests to CO2-induced climate change. *Nature Geoscience,* **6**,
903 268-273.
904 Irion G (1978) Soil infertility in the Amazonian rain forest. *Naturwissenschaften,* **65**,
905 515-519.
906 Krinner G, Viovy N, De Noblet-Ducoudré N *et al.* (2005) A dynamic global
907 vegetation model for studies of the coupled atmosphere-biosphere system.
908 *Global Biogeochemical Cycles,* **19**, GB1015.
909 Kucharik CJ, Foley JA, Delire C *et al.* (2000) Testing the performance of a Dynamic
910 Global Ecosystem Model: Water balance, carbon balance, and vegetation
911 structure. *Global Biogeochemical Cycles*, **14**, 795–825.
912 Lewis SL, Phillips OL, Sheil D *et al.* (2004) Tropical forest tree mortality,
913 recruitment and turnover rates: calculation, interpretation and comparison
914 when census intervals vary. *Journal of Ecology*, **92**, 929-944.
915 Lewis SL (2006) Tropical forests and the changing earth system. *Philosophical*
916 *Transactions of the Royal Society of London (Series B),* **361**, 195-210.
917 Lopez-Gonzalez G, Lewis SL, Burkitt M, Phillips OL (2011) ForestPlots.net: a new
918 web application and research tool to manage and analyse tropical forest plot
919 data. *Journal of Vegetation Science,* **22**, 610-613.
920 Lopez-Gonzalez G, Lewis SL, Burkitt M, Baker TR, Phillips OL (2012)
921 ForestPlots.net Database. www.forestplots.net. Date of extraction 01.09.13

922 Lopez-Gonzalez G, Mitchard ETA, Feldpausch TR *et al.* (2014) Amazon forest
923 biomass measured in inventory plots. Plot Data from "Markedly divergent
924 estimates of Amazon forest carbon density from ground plots and satellites",
925 ForestPlots.NET DOI: 10.5521/FORESTPLOTS.NET/2014_1
926 Mahowald N, Kohfeld K, Hansson M *et al.* (1999) Dust sources and deposition during
927 the last glacial maximum and current climate: A comparison of model results
928 with paleodata from ice cores and marine sediments. *Journal of Geophysical*
929 *Research: Atmospheres (1984–2012),* **104**, 15895-15916.
930 Mahowald NM, Artaxo P, Baker AR, Jickells TD, Okin GS, Randerson JT, Townsend
931 AR (2005) Impacts of biomass burning emissions and land use change on
932 Amazonian atmospheric phosphorus cycling and deposition. *Global*
933 *Biogeochemical Cycles,* **19**, GB4030.
934 Malhi Y (2012) The productivity, metabolism and carbon cycle of tropical forest
935 vegetation. *Journal of Ecology,* **100**, 65-75.
936 Malhi Y, Aragao LEO, Metcalfe DB *et al.* (2009) Comprehensive assessment of
937 carbon productivity, allocation and storage in three Amazonian forests. *Global*
938 *Change Biology,* **15**, 1255-1274.
939 Malhi Y, Baker TR, Phillips OL *et al.* (2004) The above-ground coarse wood
940 productivity of 104 Neotropical forest plots. *Global Change Biology,* **10**, 563-
941 591.
942 Malhi Y, Doughty CE, Goldsmith GR *et al.* (2015) The linkages between
943 photosynthesis, productivity, growth and biomass in lowland Amazonian
944 forests. *Global Change Biology*, **21**, 2283-2295.

945 Malhi Y, Wood D, Baker TR *et al.* (2006) The regional variation of above-ground
946 live biomass in old-growth Amazonian forests. *Global Change Biology,* **12**,
947 1107-1138.
948 Malhi YM, Meir P, Brown S (2002) Forest, carbon and global climate. *Philosophical*
949 *Transactions of the Royal Society (Series B),* **360**, 1567-1591.
950 Marimon BS, Marimon-Junior BH, Feldpausch TR *et al.* (2014) Disequilibrium and
951 hyperdynamic tree turnover at the forest–cerrado transition zone in southern
952 Amazonia. *Plant Ecology & Diversity,* **7**, 281-292.
953 Marthews T, Quesada C, Galbraith D, Malhi Y, Mullins C, Hodnett M, Dharssi I
954 (2014) High-resolution hydraulic parameter maps for surface soils in tropical
955 South America. *Geoscientific Model Development,* **7**, 711-723.
956 Mitchard ET, Feldpausch TR, Brienen RJ *et al.* (2014) Markedly divergent estimates
957 of Amazon forest carbon density from ground plots and satellites. *Global*
958 *Ecology and Biogeography*, **23**, 935-946.
959 Muller-Landau HC, Condit RS, Chave J *et al.* (2006) Testing metabolic ecology
960 theory for allometric scaling of tree size, growth and mortality in tropical
961 forests. *Ecology Letters,* **9**, 575-588.
962 Negrón-Juárez RI, Koven CD, Riley WJ *et al.* (2015) Observed allocations of
963 productivity and biomass, and turnover times in tropical forests are not
964 accurately represented in CMIP5 Earth system models. *Environmental*
965 *Research Letters* **10**, 064017.
966 Nepstad DC, Marisa Tohver I, Ray D, Moutinho P, Cardinot G (2007) Mortality of
967 large trees and lianas following experiemental drought in an Amazon forest.
968 *Ecology,* **88**, 2259-2269.

969 Pan Y, Birdsey RA, Fang J *et al.* (2011) A large and persistent carbon sink in the
970 world's forests. *Science,* **333**, 988-993.
971 Pebesma EJ (2004) Multivariable geostatistics in S: the *gstat* package. *Computers &*
972 *Geosciences*, **30**, 683-691.
973 Penman J, Gytarsky M, Hiraishi T *et al.* (2003) *Good practice guidance for land use,*
974 *land-use change and forestry*, Institute for Global Environmental Strategies.
975 Phillips OL, Aragão L, Fisher JB *et al.* (2009) Drought sensitivity of the Amazon
976 rainforests. *Science,* **323**, 1344-1347.
977 Phillips OL, Baker TR, Arroyo L *et al.* (2004) Pattern and process in Amazon tree
978 turnover, 1976-2001. *Philosophical Transactions of the Royal Society of*
979 *London Series B-Biological Sciences,* **359**, 381-407.
980 Pinheiro J, Bates D, DebRoy S, Sarkar D and R Core Team (2015). nlme: Linear and
981 Nonlinear Mixed Effects Models. R package version 3.1-122, http://CRAN.
982 Quesada C, Lloyd J, Schwarz M *et al.* (2010) Variations in chemical and physical
983 properties of Amazon forest soils in relation to their genesis. *Biogeosciences,*
984 **7**, 1515-1541.
985 Quesada CA, Phillips OL, Schwarz M *et al.* (2012) Basin-wide variations in Amazon
986 forest structure and function are mediated by both soils and climate
987 *Biogeosciences,* **9**, 2203-2246.
988 R Development Core Team (2012) *R: A Language and Environment for Statistical*
989 *Computing,* Vienna, R Foundation for Statistical Computing.
990 Rammig A, Jupp T, Thonicke K *et al.* (2010) Estimating the risk of Amazonian forest
991 dieback. *New Phytologist,* **187**, 694-706.
992 Restrepo-Coupe N, da Rocha HR, Hutyra LR *et al.* (2013) What drives the seasonality
993 of photosynthesis across the Amazon basin? A cross-site analysis of eddy flux

tower measurements from the Brasil flux network. *Agricultural and Forest Meteorology*, **182–183**, 128-144.

Rowland L, Da Costa A, Galbraith DR *et al.* (2015). Death from drought in tropical forests is triggered by hydraulics not carbon starvation. *Nature*, **528**, 119-122.

Sakschewski B, Von Bloh W, Boit A *et al.* (2015) Leaf and stem economics spectra drive functional diversity in a dynamic global vegetation model. *Global Change Biology*, **21**, 2711-2725

Sheffield J, Goteti G, Wood EF (2006) Development of a 50-year high-resolution global dataset of meteorological forcings for land surface modeling. *Journal of Climate,* **19**, 3088-3111.

Sheil D, May RM (1996) Mortality and recruitment rate evaluations in heterogeneous tropical forests. *Journal of Ecology,* **84**, 91-100.

Sitch S, Smith B, Prentice IC *et al.* (2003) Evaluation of ecosystem dynamics, plant geography and terrestrial carbon cycling in the LPJ dynamic global vegetation model. *Global Change Biology,* **9**, 161-185.

Talbot J, Lewis SL, Lopez-Gonzalez G *et al.* (2014) Methods to estimate aboveground wood productivity from long-term forest inventory plots. *Forest Ecology and Management,* **320**, 30-38.

Ter Steege H, Pitman N, Phillips OL *et al.* (2006) Continental scale patterns of canopy tree composition and function across Amazonia. *Nature,* **443**, 444-447.

Verbeeck H, Peylin P, Bacour C, Bonal D, Steppe K, Ciais P (2011) Seasonal patterns of CO2 fluxes in Amazon forests: Fusion of eddy covariance data and the ORCHIDEE model. *Journal of Geophysical Research: Biogeosciences (2005–2012),* **116**.

1018 Wang X, Piao S, Ciais P *et al.* (2014) A two-fold increase of carbon cycle sensitivity
1019 to tropical temperature variations. *Nature,* **506**, 212-215.
1020 Weng ES, Malyshev S, Lichstein JW *et al.* (2015). Scaling from individual trees to
1021 forests in an Earth system modeling framework using a mathematically
1022 tractable model of height-structured competition. *Biogeosciences*, **12,** 2655-
1023 2694.
1024 Zanne AE, Lopez-Gonzalez G, Coomes DA *et al.* (2009) Global wood density
1025 database. *Dryad Identifier: http://hdl. handle. net/10255/dryad*, *235*.
1026 Zhang K, Almeida Castanho AD, Galbraith DR *et al.* (2015) The fate of Amazonian
1027 ecosystems over the coming century arising from changes in climate,
1028 atmospheric CO_2, and land use. *Global Change Biology*, **21**, 2569-2587.
1029 Zhao M, Running SW (2010) Drought-induced reduction in global terrestrial net
1030 primary production from 2000 through 2009. *Science,* **329**, 940-943.